

RESEARCH

Open Access



# Phosphorylated A $\beta$ peptides in human Down syndrome brain and different Alzheimer's-like mouse models

Sathish Kumar<sup>1,2</sup>, Cynthia A. Lemere<sup>2\*†</sup> and Jochen Walter<sup>1\*†</sup> 

## Abstract

The deposition of neurotoxic amyloid- $\beta$  (A $\beta$ ) peptides in extracellular plaques in the brain parenchyma is one of the most prominent neuropathological features of Alzheimer's disease (AD), and considered to be closely related to the pathogenesis of this disease. A number of recent studies demonstrate the heterogeneity in the composition of A $\beta$  deposits in AD brains, due to the occurrence of elongated, truncated and post-translationally modified A $\beta$  peptides that have peculiar characteristics in aggregation behavior and biostability. Importantly, the detection of modified A $\beta$  species has been explored to characterize distinct stages of AD, with phosphorylated A $\beta$  being present in the clinical phase of AD. People with Down syndrome (DS) develop AD pathology by 40 years of age likely due to the overproduction of A $\beta$  caused by the additional copy of the gene encoding the amyloid precursor protein on chromosome 21. In the current study, we analysed the deposition of phosphorylated and non-phosphorylated A $\beta$  species in human DS, AD, and control brains. In addition, deposition of these A $\beta$  species was analysed in brains of a series of established transgenic AD mouse models using phosphorylation-state specific A $\beta$  antibodies. Significant amounts of A $\beta$  phosphorylated at serine residue 8 (pSer8A $\beta$ ) and unmodified A $\beta$  were detected in the brains of DS and AD cases. The brains of different transgenic mouse models with either only human mutant amyloid precursor protein (APP), or combinations of human mutant APP, Presenilin (PS), and tau transgenes showed distinct age-dependent and spatiotemporal deposition of pSer8A $\beta$  in extracellular plaques and within the vasculature. Together, these results demonstrate the deposition of phosphorylated A $\beta$  species in DS brains, further supporting the similarity of A $\beta$  deposition in AD and DS. Thus, the detection of phosphorylated and other modified A $\beta$  species could contribute to the understanding and dissection of the complexity in the age-related and spatiotemporal deposition of A $\beta$  variants in AD and DS as well as in distinct mouse models.

**Keywords:** Alzheimer's disease, Amyloid  $\beta$  peptide, Cerebral amyloid angiopathy, Down syndrome, Modified A $\beta$ , Mouse models, Phosphorylation, Post-translational modification

\* Correspondence: [clemere@bwh.harvard.edu](mailto:clemere@bwh.harvard.edu); [Jochen.Walter@ukbonn.de](mailto:Jochen.Walter@ukbonn.de)

<sup>†</sup>Cynthia A. Lemere and Jochen Walter contributed equally to this work.

<sup>2</sup>Ann Romney Center for Neurologic Diseases, Brigham and Women's Hospital, Harvard Medical School, Boston, MA 02115, USA

<sup>1</sup>Department of Neurology, University of Bonn, 53127 Bonn, Germany



© The Author(s). 2020 **Open Access** This article is licensed under a Creative Commons Attribution 4.0 International License, which permits use, sharing, adaptation, distribution and reproduction in any medium or format, as long as you give appropriate credit to the original author(s) and the source, provide a link to the Creative Commons licence, and indicate if changes were made. The images or other third party material in this article are included in the article's Creative Commons licence, unless indicated otherwise in a credit line to the material. If material is not included in the article's Creative Commons licence and your intended use is not permitted by statutory regulation or exceeds the permitted use, you will need to obtain permission directly from the copyright holder. To view a copy of this licence, visit <http://creativecommons.org/licenses/by/4.0/>. The Creative Commons Public Domain Dedication waiver (<http://creativecommons.org/publicdomain/zero/1.0/>) applies to the data made available in this article, unless otherwise stated in a credit line to the data.

## Introduction

Depositions of amyloid- $\beta$  ( $A\beta$ ) peptides as senile plaques in the brain parenchyma and in the walls of cerebral blood vessels are common neuropathological features of the Alzheimer's disease (AD) [1–3].  $A\beta$  peptides derive from the proteolytic processing of the amyloid precursor protein (APP) by proteases called  $\beta$ - and  $\gamma$ -secretase [4–6]. In addition to the generation and deposition of well-characterized  $A\beta_{40}$  and  $A\beta_{42}$  amino acid length variants, recent studies also showed the occurrence of several N- and C-terminally truncated or elongated  $A\beta$  species that result from alterations in the cleavage by  $\beta$ - and  $\gamma$ -secretase or alternative processing by other proteases [7–13]. Additional heterogeneity in  $A\beta$  peptides comes from a number of post-translational modifications that are also found in characteristic  $A\beta$  deposits in parenchymal extracellular plaques and cerebral amyloid angiopathy (CAA) [14–22]. N- and C-terminal truncated or elongated species as well as post-translationally modified  $A\beta$  have specific characteristics in aggregation and biostability [23–28].

Down syndrome is a genetic disorder caused by an extra copy of chromosome 21, and characterized by specific facial and neurological features. People with DS also have an increased risk of developing early onset AD [29–31]. Interestingly the gene encoding APP is localized within a region of chromosome 21 that is critical for DS, and the triplication of the *APP* gene results in elevated levels of  $A\beta$  peptides that form amyloid plaques at least two decades prior to the onset of the clinical AD-like symptoms [31–33]. DS brains demonstrate  $A\beta$  plaques already at 12–30 year of age, principally in the form of diffuse  $A\beta$  plaques, the type of early  $A\beta$  pathology also seen at pre-clinical (i.e., pathological aging) and prodromal stages of sporadic AD [30, 34–36]. In DS subjects, aged > 40 years, levels of cortical  $A\beta$  deposition are similar to those observed in sporadic, late onset AD and demonstrate cored neuritic plaques, which are of neuropathological diagnostic significance in AD [29–31]. Notably, autopsy studies of DS brain show the occurrence of isomerized, racemized, truncated, pyroglutamate and oxidized  $A\beta$ , indicating the accumulation of post-translationally modified  $A\beta$  variants as reviewed previously [30].

We recently showed that  $A\beta$  undergoes phosphorylation at serine residue 8, which affects its conformation, aggregation, neurotoxicity and proteolytic degradation [18, 25, 27, 37, 38]. Phosphorylated Ser8- $A\beta$  (pSer8 $A\beta$ ) occurs in vivo in the brains of human AD patients, non-human primates and canines [39–42]. Notably, the detection of pSer8 $A\beta$ , together with pyroglutamate modified  $A\beta$  in brain sections or brain extracts has recently been explored to establish a staging system for AD pathology based on the sequential deposition of these modified  $A\beta$  variants during the pathogenesis of AD [42]. While pyroglutamate modified  $A\beta$  could already be

detected in the pre-clinical stage of AD, pSer8 $A\beta$  species occur selectively in the clinical phase of AD. These findings support a role of modified  $A\beta$  species in the pathobiology of AD.

Murine models are crucial for the advancement of our understanding of  $A\beta$  deposition in AD. Several transgenic mouse models have been generated that overexpress APP with or without familial Alzheimer disease (FAD) mutations or combinations of human mutant APP, PS, and tau transgenes that reflect certain aspects of human AD [43–47]. These AD mouse models are immensely important for the investigation of AD related pathophysiological processes.

Here, we analysed the occurrence of pSer8 $A\beta$  in the brains of DS cases, and in different single, double and triple transgenic mouse models of AD. Our data demonstrate the deposition of phosphorylated  $A\beta$  in DS cases thereby further supporting the similarity of  $A\beta$  lesions in DS and AD. pSer8 $A\beta$  was also found in all transgenic mouse models analysed and showed characteristic age-dependent, and spatiotemporal deposition. Together, these results indicate that deposition of pSer8 $A\beta$  is a common feature of pathological  $A\beta$  deposition in the human brain, and could be further explored to dissect the composition of  $A\beta$  lesions in different transgenic mouse models.

## Material and methods

### Human subjects

We used phosphorylation-state specific monoclonal antibodies to characterize the deposition of phosphorylated (pSer8 $A\beta$ ) and non-phosphorylated (np $A\beta$ ) variants of  $A\beta$  in 3 DS (46, 47 and 55 years), 12 sporadic AD (average,  $86 \pm 7$  years) and 8 non-demented aged control (AC; average,  $67 \pm 10$  years) brains (Table 1). Human brain tissue was collected at the time of autopsy, having obtained prior consent from the next of kin and following protocols approved by the Partners Human Research Committee at Brigham and Women's Hospital (Boston, MA, USA). Human cortical and hippocampal brain blocks of AC, AD and DS were fixed in 10% neutral buffered formalin for two hours (brief fixation) with the exception of one DS brain (47 years old) that was fixed for about 1 month (routine fixation) before undergoing washing in PBS and paraffin processing. Human subject information including age, gender, and brain region examined (frontal, occipital, parietal, temporal/hippocampal, hippocampal) and semi-quantitative staining results for this study are summarized in Table 1.

### Transgenic AD mouse models

Mouse brain tissue was obtained from six transgenic mouse lines that are commonly used as AD models,

**Table 1** Examination summary of aged control (AC), Alzheimer's disease (AD) and Down syndrome (DS) brains

Cases	Age (years)	Gender	Brain region examined	82E1 (A $\beta$ 1-x)	7H3D6 (npA $\beta$ )	1E4E11 (pSerA $\beta$ )	PMI (hours)	Brain weight (grams)	Cause of Death	Braak Stage
<b>Aged Control (AC)</b>										
AC-1	72	Female	F	-	-	-	NA	1300	Cardiac arrest	NA
			HC	+	+	(+)				
AC-2	53	Male	F	-	-	-	9	1500	Cardiac arrest	NA
			HC	+	-	-				
AC-3	60	Female	F	+++	-	-	11	1150	Cardiac arrest; Sepsis	NA
			O	+++	-	-				
AC-4	64	Male	HC	+++	+	-	9.5	1380	Congestive heart failure	NA
AC-5	70	Male	F	++	+	(+)	17	1500	Mesothelia carcinoma	NA
			HC	+++	+	+				
AC-6	60	Female	F	++	-	-	3.5	1380	COPD; AS	NA
			HC	++	-	-				
AC-7	87	Female	F	+++	+	(+)	NA	NA	Choking	NA
			T/HC	-	-	-				
AC-8	74	Male	F	++	-	-	NA	1400	Dead on Arrival	NA
<b>Alzheimer's Disease (AD)</b>										
AD-1	82	Female	F	++++	+	++	16	900	Pneumonia	NA
			HC	+++	+	++				
AD-2	79	Female	F	+++	++	+	13	1040	AD; AS	NA
			HC	+++	+	++				
AD-3	91	Female	T	++	+	-	3.5	1370	Pneumonia; AD; AS; Lacunar infarct	III -IV
			HC	+++	+	++				
AD-4	71	Male	F	+++	+	++	36	NA	AD; AS	NA
			HC	+++	+	++				
AD-5	84	Female	F	+++	-	++	NA	1000	AD; AS; Binswanger	NA
			T	++	++	-				
AD-6	92	Female	HC	+++	+	++	7	1210	AD; AS; Infarct	NA
AD-7	78	Male	F	+++	+	++	18	1200	AD; AS	V-VI
			HC	++	-	+				
AD-8	96	Female	F	++	++	++	21	1050	AD; AS; Infarct	NA
			HC	+++	+	++				
AD-9	78	Male	P	+	++	+	NA	1180	AD; Subdural hematoma	V-VI
			T/HC	+++	+++	+				
AD-10	88	Female	P	+++	+	+	24	1220	AD; AS	
			HC F	++++	++	+++				
AD-11	84	Female	F	+++	-	++	16.5	1110	AD; AS; DLBD	NA
			HC	+++	+	++				
AD-12	88	Female	F	+++	+	+	24	1050	AD; AS; Infarct	V-VI
			HC	++	++	+				
<b>Down syndrome (DS)</b>										
DS-1	47	Male	F	++++	+	++	34	910	Glioblastoma; AD	NA
			T/HC	++++	+	++				

**Table 1** Examination summary of aged control (AC), Alzheimer's disease (AD) and Down syndrome (DS) brains (*Continued*)

Cases	Age (years)	Gender	Brain region examined	82E1 (A $\beta$ 1-x)	7H3D6 (npA $\beta$ )	1E4E11 (pSerA $\beta$ )	PMI (hours)	Brain weight (grams)	Cause of Death	Braak Stage
DS-2	55	Male	F	++++	++	++	NA	1040	Pneumonia; AD	NA
			T	++++	++	+++				
DS-3	46	Female	T/HC	+++	++	++	18	870	Pneumonia; AD	NA

The following semi-quantitative scoring criteria were used: -, no staining; (+), 1–10 plaques; +, 11–30 plaques; ++, 31–50 plaques; +++, 51–100 plaques, and +++++, > 100 plaques per cm<sup>2</sup>. F frontal; HC hippocampal; T temporal; O occipital; P parietal; DLBD Diffuse Lewy Body Disease; COPD Chronic Obstructive Pulmonary Disease; AS Arteriolar sclerosis; NA not available

namely J20 [48], hAPP751 [49], TgSwDI [50], APP/PS1 $\Delta$ E9 [51], PS/APP [52], and 3xTg-AD [53] (Table 2). Hemibrains were fixed in 10% formalin or 4% paraformaldehyde for 2 to 24 h before being processed for paraffin embedding and then sectioned at 10  $\mu$ m. All use of mice at Brigham and Women's Hospital was approved by the Harvard Medical Area Standing Committee on animals and was in compliance with state and federal regulations.

### Immunohistochemistry

Immunohistochemistry was performed on 8–10  $\mu$ m thick sections of hippocampus and cortex as previously described [20, 41], using three different primary antibodies. In brief, human brain sections were deparaffinized in two changes of Histo-Clear (National Diagnostics, Atlanta, GA) and rehydrated in graded ethanol solutions. Endogenous peroxidase activity was quenched with 0.3% H<sub>2</sub>O<sub>2</sub> in methanol for 10 min. All

**Table 2** Transgenic AD-like mouse models in which pSer8A $\beta$  and npA $\beta$  deposition has been analyzed. APP, Amyloid precursor protein; PS1, Presenilin-1; h-human; m-mouse; Swe, Swedish; Ind, Indiana; Lon, London; PSEN1, Presenilin-1; KI, Knock-in; Tg, Transgenic; Ref, Reference

Mouse model	Transgene	Ref.	Transgenic promoter	Age (months)	Amyloid plaques		CAA lesions		
					npA $\beta$	pSer8A $\beta$	npA $\beta$	pSer8A $\beta$	
<b>APP Transgenics:</b>									
J20	hAPP770 (K670N/M671L; V717F) Swe; Ind mutation	48	<i>PDGFB</i>	4 (n = 4)	+	-	No	No	
				8 (n = 4)	++	+	Yes	Yes	
				16 (n = 3)	++++	+++	Yes	Yes	
hAPP751	hAPP751 (K670N/M671L; V717I) Swe; Lon mutation	49	mouse <i>Thy-1</i>	14 (n = 2)	++++	+++	Yes	Yes	
				TgSwDI	hAPP770 (K670N/M671L; E693Q; D694N) Swe; Dutch; Iowa mutation	50	mouse <i>Thy-1</i>	3 (n = 4)	+
6 (n = 2)	++	+	Yes	Yes					
12 (n = 4)	+++	++	Yes	Yes					
24 (n = 4)	++++	+++	Yes	Yes					
<b>APP/PS1 Transgenics:</b>									
APP/PS1 $\Delta$ E9	m/hAPP695 (K595N/M596L); hPS1 deletion of exon 9 Swe; PSEN1 $\Delta$ E9	51	mouse <i>PrnP</i>	6 (n = 4)	++	+	Yes	Yes	
				17 (n = 3)	+++	++	Yes	Yes	
				24 (n = 4)	++++	+++	Yes	Yes	
PS/APP	hAPP695 hPS1 (M146L) Swe; PS1M146L	52	Hamster <i>PrnP</i> (APP) <i>PDGFB</i> (PS1)	18 (n = 5)	++++	+++	Yes	Yes	
<b>APP/PS1/Tau Transgenics:</b>									
3xTg-AD	hAPP695 (K670N/M671L); hPS1 (M146V); TauP301L Swe;PS1M146V;MAPT4R0N (P301L)	53	mouse <i>Thy-1.2</i> (APP, Tau) PS1 KI	5 (n = 4)	++	+	No	No	
				14 (n = 3)	+++	++	Yes	Yes	
				27 (n = 4)	++++	+++	Yes	Yes	

The following semi-quantitative scoring criteria were used: -, no plaque staining, +, 1–5 plaques; ++, 6–10 plaques; +++, 11–100 plaques; +++++, > 100 plaques. Abbreviations: Ref References; Swe Swedish; Ind Indiana; Lon London; PS1 presenilin-1, MAPT, microtubule-associated protein tau; PDGFB platelet-derived growth factor B-chain; PrnP prion protein; KI, knock-in

paraffin sections were pretreated with 88% formic acid for 8 min to increase recognition of antigen binding sites. Sections were subsequently washed with water for 10 min and incubated with primary antibody overnight at 4 °C. After incubation for 30 min at room temperature with a biotinylated secondary antibody (Vector Laboratories). Immunoreactivity was visualized with the VEC-TASTAIN Elite horseradish peroxidase ABC kit (Vector Laboratories) and DAB (Sigma-Aldrich) as chromogen.

When using mouse monoclonal antibodies on mouse brain sections, a Mouse on Mouse (M.O.M.) kit (Vector Laboratories) was used to inhibit nonspecific background staining. The mouse monoclonal antibody (mAb) 82E1 (dilution 1:500; Immuno-Biological Laboratories, Japan) recognizes A $\beta$  peptides starting at aspartic acid 1 (A $\beta$ 1-x). The murine 1E4E11 mAb (dilution 1:500 - pSer8A $\beta$ ) is reactive to A $\beta$  peptides phosphorylated at Ser8, and rat 7H3D6 mAb (dilution 1:500 - npA $\beta$ ) specifically recognizes A $\beta$  peptide with Ser8 in a non-phosphorylated state [37]. The specificity of the phosphorylation-state specific antibodies 1E4E11 and 7H3D6 was demonstrated previously by pre-adsorption with synthetic A $\beta$  peptides with Ser8 in phosphorylated or non-phosphorylated state by western immunoblotting and immunohistochemistry and by staining with secondary antibodies alone [37, 39]. Semi-quantitative analysis was performed by scoring immunoreactivity of each antibody by a person blinded to the diagnosis associated with each brain sample. Sets of immunostained serial sections from AC, AD and DS cases were photographed, and the number of only distinct plaques, both the diffuse and compact types within the region of interest was analyzed using ImageJ image processing and analysis software (National Institutes of Health, Bethesda, USA). Gray scale thresholding was used to identify positively stained structures from background staining. Operator editing was used to remove staining artifacts. For human brain tissues, the number of npA $\beta$  and pSer8A $\beta$ -immunopositive plaques in specific brain regions was semi-quantitatively scored as: -, no staining; (+), 1–10 plaques; +, 11–30 plaques; ++, 31–50 plaques; +++, 51–100 plaques, and +++++, > 100 plaques per cm<sup>2</sup>. For transgenic mouse samples, semi-quantitative analysis of total npA $\beta$  and pSer8A $\beta$  immunoreactivity was performed using Bioquant image analysis software, which allows identification of objects based on thresholding of the optical density to identify A $\beta$  deposits. The threshold of detection was held constant during analysis, and the imager was blinded to the study. 4–6 sections per mouse were analysed by counting the number of npA $\beta$  and pSer8A $\beta$  positive plaques in the entire hippocampus and cortex. The analysed areas were kept constant for all sections. Plaque scoring of each group is determined by calculating the sum of individual scores divided by the number of animals per group. Scoring key: -, no plaque

staining; +, 1–5 plaques; ++, 6–10 plaques; +++, 11–100 plaques; +++++, > 100 plaques per area. Images were captured in a single session using a constant threshold under a Nikon Eclipse E400 microscope.

## Results

Human hippocampal brain sections were stained with monoclonal antibodies specifically recognizing the N-terminus of A $\beta$  starting at amino acid Asp1 (A $\beta$ 1-x) (Fig. 1a, d and g), with monoclonal antibodies specifically recognizing A $\beta$  with Ser8 in phosphorylated (pSer8A $\beta$ ) (Fig. 1c, f and i, supplementary Fig. 1) or non-phosphorylated state (non-phospho A $\beta$ ; npA $\beta$ ) (Fig. 1b, e and h, supplementary Fig. 1) to assess A $\beta$  deposition in 3 DS, 12 AD and 8 AC brains. Results of a semi-quantitative analysis of A $\beta$ 1-x, pSer8A $\beta$  and npA $\beta$  deposition in extracellular plaques are summarized in Table 1. Figure 1 shows immunoreactivity of A $\beta$ 1-x, npA $\beta$  and pSer8A $\beta$  deposits in hippocampus of a 60-year-old female AC (Fig. 1a-c), a 47-year-old male DS individual (Fig. 1d-f) and an 88-year-old female AD patient (Fig. 1g-i). pSer8A $\beta$  was present in extracellular A $\beta$  plaques in all three DS cases, and all AD cases (Table 1).

The 3 DS cases had abundant deposits of A $\beta$ 1-x also containing pSer8A $\beta$  and npA $\beta$  peptides (Table 1, Fig. 1d-f). In all 3 DS brains, extracellular plaques were found in the hippocampus, the frontal cortex as well as in the temporal cortex. Overall, there was an overlap in the immunoreactivity for pSer8A $\beta$  and A $\beta$  variants starting with Asp1 of the A $\beta$  sequence (A $\beta$ 1-x; Fig. 1d and f). Immunostaining with 7H3D6 mAb detected fewer plaques in DS brains (Fig. 1e; Table 1). It is important to note that the 7H3D6 antibody does not detect A $\beta$  species modified by N-terminal truncation (A $\beta$ 3–42), pyroglutamate formation (pyroGluA $\beta$ 3–42), nitration (3NTyr10-A $\beta$ ) or phosphorylation at Ser8 (pSer8A $\beta$ ) (Supplementary Fig. 1). It is therefore possible that beside phosphorylation, the presence of other modifications and truncation of A $\beta$  also contributes to the decreased reactivity of the monoclonal antibody 7H3D6 in these samples. Indeed, abundant levels of aminoterminaly modified and truncated A $\beta$  peptides have been detected in DS brains previously [30, 35, 36, 54, 55].

All AD brains showed robust A $\beta$  deposits (Table 1), that were also detected by the pSer8A $\beta$  specific antibody 1E4E11 (Fig. 1g, i). A $\beta$  plaques in AD cases were predominantly found in the frontal cortex and contained both pSer8A $\beta$  and npA $\beta$  variants (Table 1). All 8 control (AC) brains showed A $\beta$ 1-x positive plaques at variable levels (Table 1, Fig. 1a-c). In contrast, pSer8A $\beta$  positive plaques were absent in 4 and only very weakly detected in the other 4 control brains, consistent with the occurrence of pSer8A $\beta$  selectively in the clinical phase of AD [39, 42]. These results indicate that deposition of

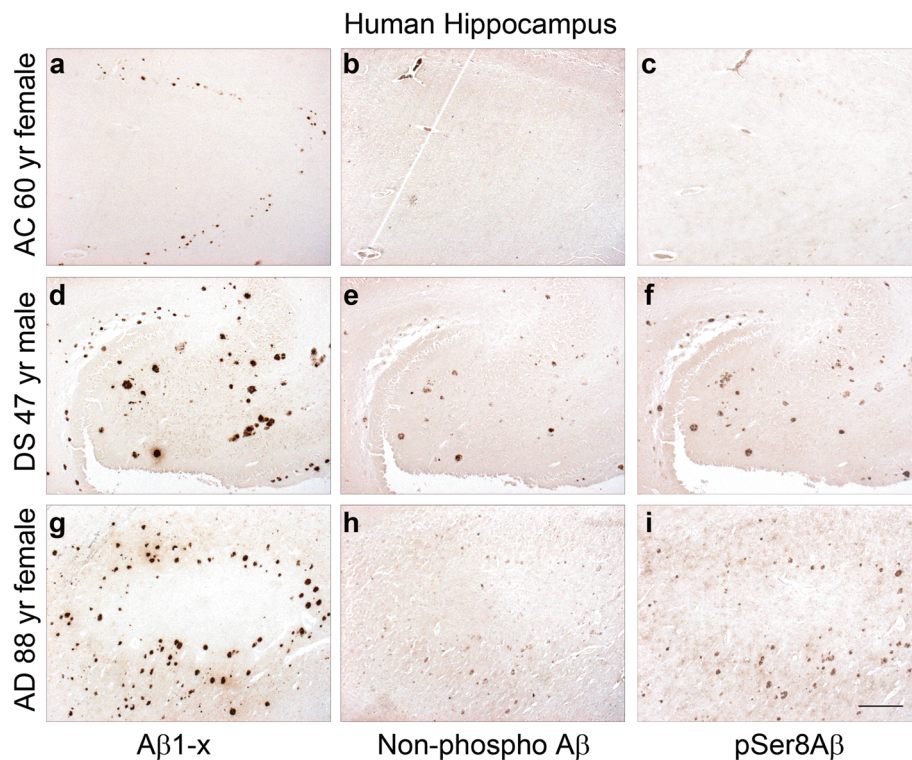


**Fig. 1** Immunohistochemical detection of pSer8A $\beta$  peptides in DS and AD brains. Immunohistochemical staining was performed on adjacent serial paraffin sections with monoclonal antibodies 82E1 (A $\beta$ 1-x), 7H3D6 (non-phosphoA $\beta$ ) and 1E4E11 (pSer8A $\beta$ ). Asp-1 A $\beta$  (A $\beta$ 1-x), npA $\beta$  and pSer8A $\beta$  species colocalized in DS (**d-f**) and AD (**g-i**) hippocampus. pSer8A $\beta$  and npA $\beta$  were detected in extracellular A $\beta$  plaques in DS and AD brains. AC brains showed some immunoreactivity with 82E1 antibody (**a**), but very limited if any reactivity with antibodies 7H3D6 (**b**) and 1E4E11 (**c**). Scale bar = 100  $\mu$ M

pSer8A $\beta$  is characteristic for symptomatic AD as well as DS cases.

We also investigated several established transgenic AD mouse models for the deposition of pSer8A $\beta$  and npA $\beta$  peptides by immunohistochemistry. Details on the different transgenes and semi-quantitative analysis of pSer8A $\beta$  and npA $\beta$  immunoreactivity in each mouse model are summarized in Table 2. The different mouse models were grouped by their AD related transgenes. The J20 [48], hAPP751 [49] and TgSwDI [50] models, express only APP transgenes with different combined familial AD mutations (Table 2). The J20 mouse model expresses the hAPP770 variant with two mutations linked to familial AD (the Swedish and Indiana mutations) under control of the *PDGF $\beta$*  promoter. A $\beta$  deposition in J20 mice starts between 4 and 5 months of age as diffuse A $\beta$  plaques in the hippocampus. By 8–10 months, these mice show progressive and widespread A $\beta$  deposition [48]. We examined the deposition of pSer8A $\beta$  and npA $\beta$  peptides at 4, 8 and 16 months of age. Only a very modest level of npA $\beta$  immunoreactivity was observed in two of the four J20 mice at 4 months of age, exclusively detected in the hippocampus (Fig. 2a, Table 2). At this age, very faint reactivity of pSer8A $\beta$  appeared in few

extracellular amyloid deposits and in some vessels (Fig. 2b, inset). At 8 months of age, J20 mice displayed more extracellular plaques. At this age most of the npA $\beta$  positive plaques in the hippocampus and cortex also contained pSer8A $\beta$  (Fig. 2c and d). At 16 months, J20 mice had substantial deposition of npA $\beta$  and pSer8A $\beta$  in the neocortex, hippocampus, and subiculum (Fig. 2e and f, Table 2). Diffuse npA $\beta$  and pSer8A $\beta$  immunoreactivity was additionally present along the molecular layer of the dentate gyrus (DGm). pSer8A $\beta$  and npA $\beta$  deposits were also detected in leptomeningeal and parenchymal blood vessels at 16 months of age (Fig. 2e and f, and Supplementary Fig. 2a-d).

A very similar distribution and high abundance of npA $\beta$  and pSer8A $\beta$  was also observed in a different mouse model that overexpresses the human APP751 isoform containing the Swedish and London mutations under control of the *Thy-1* promoter [49]. Amyloid plaques in hAPP751 mice start to develop at 3–4 months of age in the frontal cortex, and at 5–7 months, dense amyloid deposits are observed in the hippocampus, thalamus, and olfactory region [49]. At 14 months of age, brains showed strong immunoreactivity for npA $\beta$  and pSer8A $\beta$  in diffuse and compact plaques throughout the

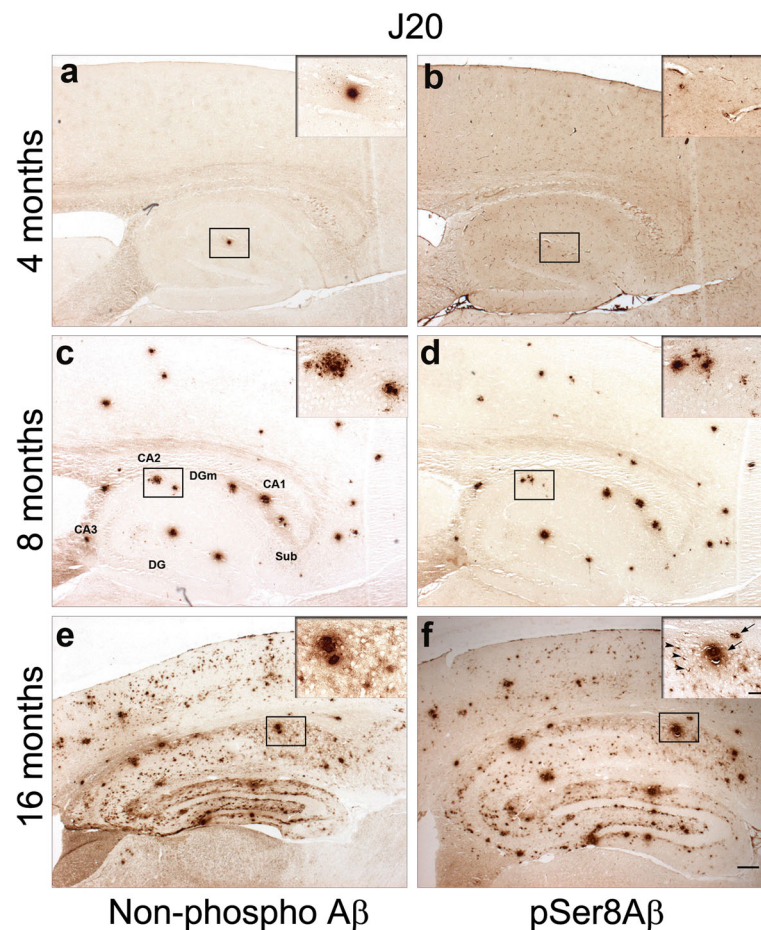


**Fig. 2** Age-dependent deposition of cerebral npA $\beta$  and pSer8A $\beta$  in J20 mice. Brain sections of 4, 8, and 16 month-old mice were immunolabeled with npA $\beta$  (**a**, **c** and **e**) and pSer8A $\beta$ -specific (**b**, **d** and **f**) antibodies. npA $\beta$  deposits were detected initially in the hippocampus at 4 months (**a**). A faint reactivity of pSer8A $\beta$  was seen in extracellular amyloid deposits and in some vessels in the hippocampus (**b**; inset). By 8 months, npA $\beta$  (**c**) and pSer8A $\beta$  deposition (**d**) extended to the neocortex as compact and diffuse deposits. By 16 months, more intense and abundant npA $\beta$  (**e**) and pSer8A $\beta$ -immunoreactivity (**f**) was observed in extracellular plaques (arrows) and blood vessels (arrowheads) affected by CAA (inset in panel **f**). Sub, subiculum; DG, dentate gyrus; DGm, dentate gyrus molecular layer. Scale bar = 200  $\mu$ m. Insets show the magnified areas indicated by the boxes. Scale bar = 50  $\mu$ m

entire hippocampus, the neocortex and thalamus, as well as in leptomeningeal and parenchymal blood vessels (Supplementary Fig. 2e-h, Table 2).

We next analysed the age-dependent deposition of npA $\beta$  and pSer8A $\beta$  in brains of TgSwDI mice that express the hAPP770 variant harboring three different APP mutations (Swedish; Dutch and Iowa) (Table 2). Notably, the A $\beta$  variants with Dutch and Iowa mutations are vasculotropic and associated with CAA [50]. As shown in Fig. 3, the TgSwDI mouse model had some of the earliest and most abundant cerebral pSer8A $\beta$  deposition, seen as extracellular diffuse plaques and vascular deposits, predominantly in the subiculum region, at 3 months of age that increased with age (Fig. 3a and b). At 6 months of age, increased A $\beta$  extracellular deposits were observed together with abundant A $\beta$  accumulation in and around blood vessels (Fig. 3c and d). At 6 months

of age, npA $\beta$  deposition was detected in the thalamus, stratum oriens, CA1, DGm, and dentate gyrus polymorphic layers (DGpl), and concomitantly increased in the subiculum (Fig. 3c). pSer8A $\beta$  immunoreactivity was observed in a subset of npA $\beta$  positive plaques in the subiculum, thalamus, and stratum oriens, and CA1 hippocampal region of the brain (Fig. 3d). At this age, only modest amounts of npA $\beta$  and pSer8A $\beta$  deposition were observed in the neocortex. By 12 months of age, A $\beta$  deposits were observed throughout the brain (Fig. 3e and f). pSer8A $\beta$  deposition was increased in the aforementioned regions and found in a subset of npA $\beta$  deposits in the hippocampal CA2 region, DGm, and neocortex (Fig. 3e and f). At 24 months of age, pSer8A $\beta$  reactivity was observed in a subset of npA $\beta$ -positive diffuse plaque-like and vascular A $\beta$  deposits (Fig. 3h) that were far more abundant in the hippocampus (specifically in the CA1,

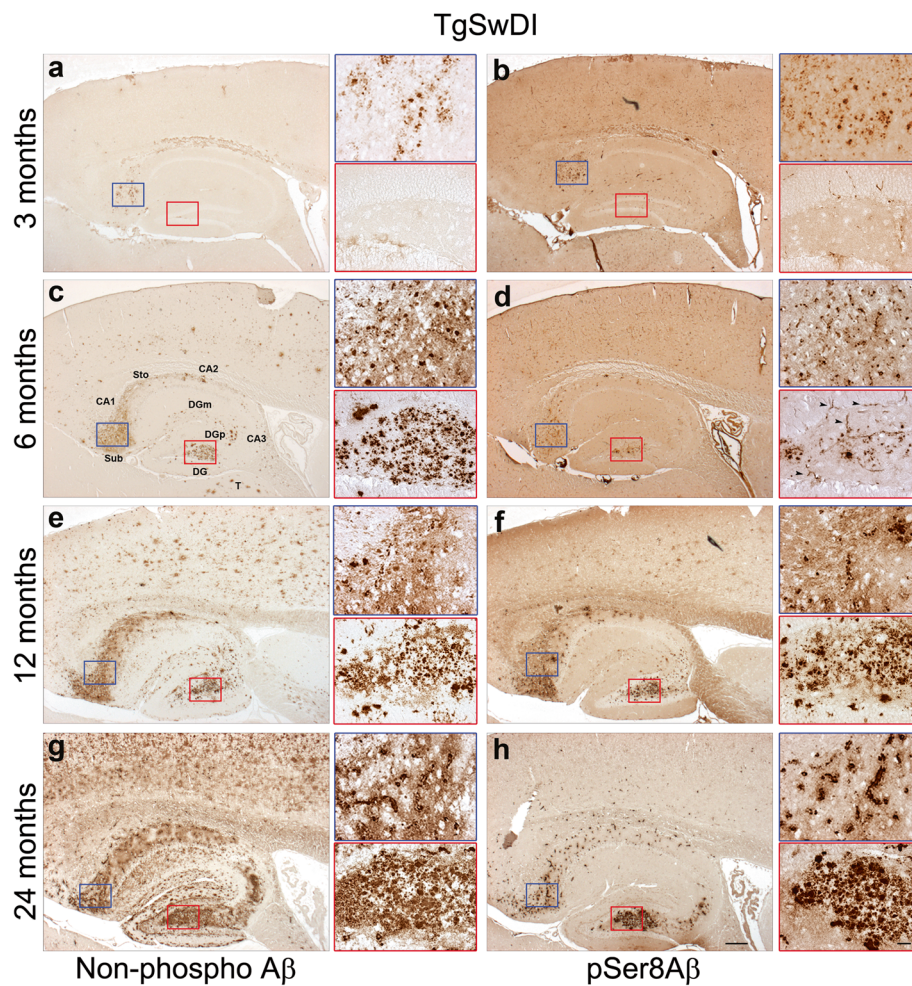


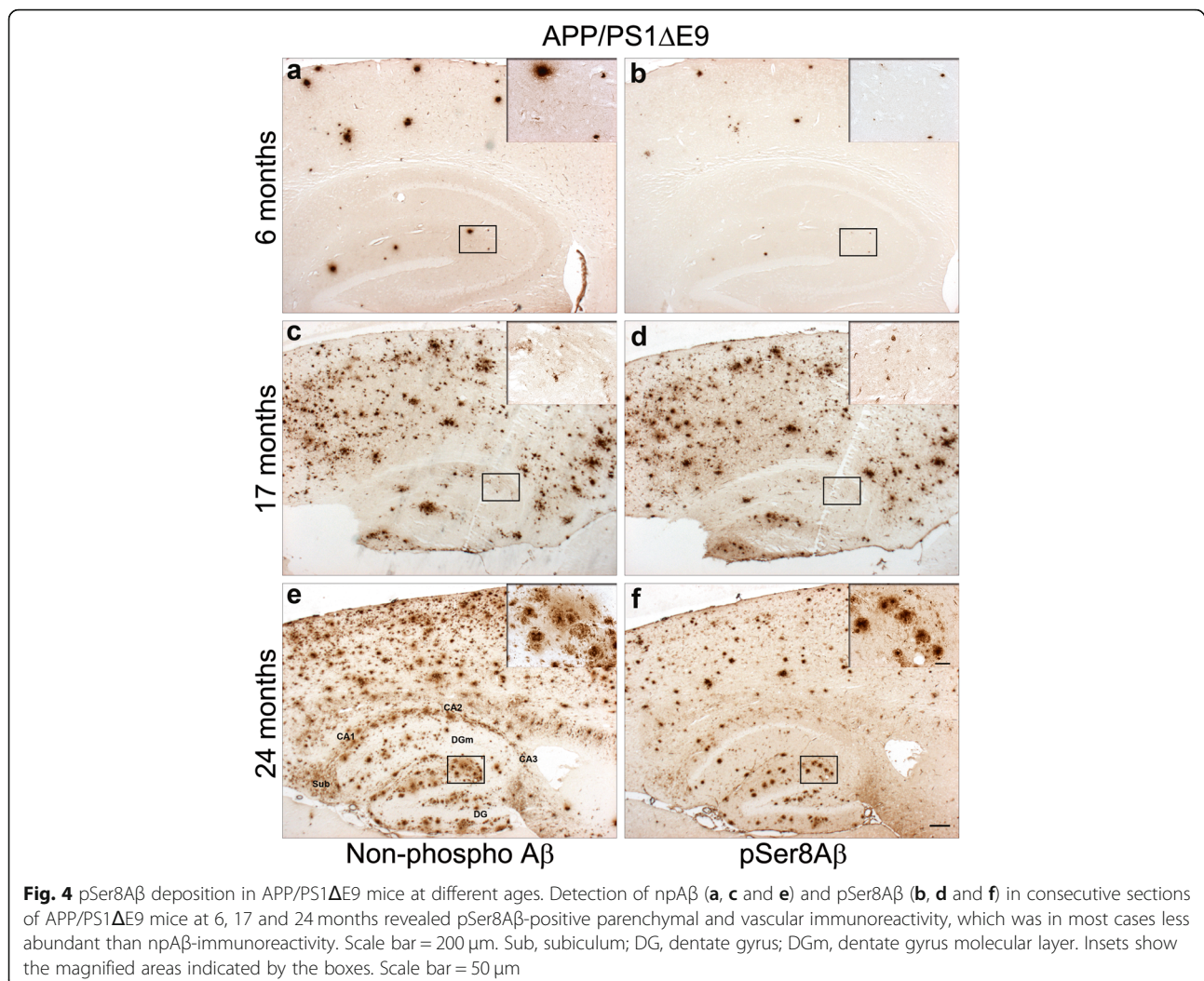
**Fig. 3** pSer8A $\beta$  deposition in TgSwDI mice at different ages in CA1 region and molecular layer of dentate gyrus (DG). Analysis of consecutive sections using npA $\beta$  and pSer8A $\beta$  antibodies in TgSwDI mice at 3, 6, 12 and 24 months of age. At 3 months, minute amounts of npA $\beta$  and pSer8A $\beta$  reactivity were seen in the subiculum (a, b). At 6 months, deposition of npA $\beta$  and pSer8A $\beta$  increased and extended to the CA1 region and dentate gyrus (c, d). By 12 months, both npA $\beta$  and pSer8A $\beta$  were increased in the vasculature between the pyramidal neurons and in the stratum oriens (e, f). By 24 months, abundant CAA was observed by intense npA $\beta$  immunoreactivity that colocalized almost completely with pSer8A $\beta$  (g, h). Sub, subiculum; Sto, stratum oriens; DG, dentate gyrus; DGm, dentate gyrus molecular layer; DGp, dentate gyrus polymorphic layer; T, thalamus. Scale bar = 200  $\mu$ m. Enlarged images (insets) in the subiculum and dentate gyrus are indicated by blue and red boxes, respectively. Scale bar = 50  $\mu$ m

CA2, CA3, DGm, DGpl, stratum oriens), the thalamus, and neocortex (Fig. 3g) compared to those found in younger mice.

In addition, we analysed two double transgenic mouse models carrying FAD associated mutations in APP and PS1 (APP<sup>swe</sup>/PS1 $\Delta$ E9 and PS1/APP mice). The APP<sup>swe</sup>/PS1 $\Delta$ E9 mice, harboring the FAD-associated Swedish mutation in APP and the exon 9 deletion in PS1 [51, 56]. This model develops plaque deposition by 6 months of age in the hippocampus and cortex. At this age, we detected npA $\beta$  positive plaques in the hippocampus and neocortex (Fig. 4a). Notably, pSer8A $\beta$  immunoreactivity was only observed in a small subset of compact plaques in the hippocampus as well as in the

neocortex in two of four mice, but not elsewhere at this age (Fig. 4b and Table 2). By 17 months, npA $\beta$ -immunopositive extracellular plaques, and vascular deposits had increased dramatically in the neocortex and hippocampus (Fig. 4c). Interestingly, APP<sup>swe</sup>/PS1 $\Delta$ E9 mice at 17 months displayed robust pSer8A $\beta$  immunoreactivity in diffuse and compact deposits in the neocortex as well as in the parenchymal blood vessels and compact deposits in the hippocampus (Fig. 4d). By 24 months, abundant npA $\beta$  immunoreactivity was noted in the hippocampus and neocortex (Fig. 4e). Most compacted plaques in the hippocampus and a subset of neocortical plaques were pSer8A $\beta$ -positive (Fig. 4f). Strong npA $\beta$  immunoreactivity was observed in leptomeningeal blood





vessels, and plaques in the molecular layer of the hippocampus that often colocalized with pSer8A $\beta$  immunoreactivity (Fig. 4e and f).

Another double transgenic mouse model with overexpression of hAPP<sup>swe</sup> and a PS1 FAD-associated mutation was generated previously by crossing APP<sup>swe</sup> (Tg2576) transgenic mice with mutant *PSEN1* (PS1M146L) expressing transgenic mice [52]. These double transgenic PS/APP mice develop A $\beta$  deposits in the cortex and hippocampus by 3 months of age that increase with aging [57]. Brains of 18 month-old mice contained abundant npA $\beta$  and pSer8A $\beta$  positive deposits (Supplementary Fig. 2i and j). npA $\beta$  appeared as extracellular plaques throughout the cortex, hippocampus, and thalamus (Supplementary Fig. 2i and k). pSer8A $\beta$  reactivity is observed in a subset of npA $\beta$ -positive extracellular plaques (Supplementary Fig. 2j and l). npA $\beta$  and pSer8A $\beta$  reactivity was also noted in vascular deposits in the parenchyma pial surface and leptomeninges (Supplementary Fig. 2i-l).

Furthermore, we analysed the brains of triple transgenic (3xTg-AD) mice possessing the Swedish APP, the PS1 M145V, and the Tau P301L mutations [53]. This model, in addition to the deposition of A $\beta$  in extracellular plaques and the formation of intraneuronal tau aggregates, also shows prominent accumulation of intraneuronal A $\beta$  immunoreactivity [53]. Examination of cortical brain sections at different ages (Table 2), revealed that npA $\beta$  and pSer8A $\beta$  immunoreactivity increased with age as intense compact deposits in different brain regions, with npA $\beta$  deposition being more abundant in extracellular deposits throughout the hippocampus and cortex (Supplementary Fig. 2m and n). Abundant intraneuronal npA $\beta$  accumulation also contained pSer8A $\beta$  immunoreactivity in neocortical regions (Supplementary Fig. 2o and p). The antibodies 7H3D6 and 1E4E11 used to detect npA $\beta$  and pSer8A $\beta$  do not crossreact with the full-length APP or its C-terminal fragments [37, 40, 42]. Thus, these data further support the pronounced

accumulation of intracellular A $\beta$  in this triple transgenic mouse model [53, 58–60].

In summary, pSer8A $\beta$  is present in all APP-overexpressing models examined in this study, and largely shows co-deposition with npA $\beta$  in extracellular plaques, blood vessels, and intraneuronal A $\beta$  aggregates, despite the specific spatiotemporal pattern of the deposits observed in the different transgenic models.

## Discussion

Using phosphorylation-state specific monoclonal antibodies, we characterized A $\beta$  pathology in human AD, AC and DS brains, and in several transgenic mouse models. Consistent with our previous findings [18, 39, 42], npA $\beta$  and pSer8A $\beta$  deposits were present in extracellular plaques of AD brains, while AC brains contained much lower amounts of npA $\beta$  and even less pSer8A $\beta$  in a subset of cases. Notably, all three DS brains also revealed the presence of npA $\beta$  and pSer8A $\beta$  in extracellular plaques. Interestingly, immunostaining with an antibody (7H3D6) that is highly specific for N-terminally unmodified A $\beta$  species (Supplementary Fig. 1) [37], resulted in only weak staining in individual AD and DS brains (Table 1). Given the high reactivity with the antibody 82E1, which specifically recognizes A $\beta$  starting at Asp1 and does not detect N-terminally truncated or pyroGlu-modified A $\beta$  species, the data could suggest that A $\beta$  species starting at Asp1 contain post-translational modifications, including phosphorylation at Ser8 or nitration of Tyr10. However, specific characteristics of the different antibodies regarding the conformation of aggregated A $\beta$  in the deposits or the processing of brain samples could also affect the detection of the different A $\beta$  species. It is important to note that, in contrast to most generic A $\beta$  antibodies used to detect A $\beta$  pathology, the monoclonal phosphorylation-state specific A $\beta$  antibodies used in the present study specifically detect A $\beta$  peptides without cross-reactivity with full-length APP and thus, allow unambiguous detection of extracellular and intracellular A $\beta$  aggregates.

In addition to the well characterized A $\beta$ 1–40/42 species, N- and C-terminally truncated or post-translationally modified forms of A $\beta$  peptides also exist in AD brains and might contribute to neurodegeneration [12, 16, 21–24, 61, 62]. Thus, detailed analyses of A $\beta$  species that constitute amyloid deposits in AD is of major interest. The DS cases demonstrated pSer8A $\beta$  reactivity in both diffuse and compact plaques that in part overlap with the immunoreactivity of npA $\beta$  and A $\beta$ 1-x variants starting with Asp1. Together with the previous demonstration of truncated A $\beta$  and pyroGlu-modified A $\beta$  peptides in AD and DS brains [20, 21, 23, 30, 36, 42, 61, 62], the detection of pSer8A $\beta$  immunoreactivity in DS brains shown here provides strong evidence for

similar mechanisms of amyloidogenesis and composition of plaques in DS and AD. Thus, it will be interesting to further investigate how the pSer8A $\beta$  species will affect senile plaque formation and other features of brain pathology in DS and AD cases. It also remains to be elucidated, which mechanisms lead to the accumulation of pSer8A $\beta$  in DS and AD. Altered expression of protein kinases and phosphatases has been described for DS and AD [63–66]. Our previous studies showed that protein kinase A (PKA) is capable to efficiently phosphorylate A $\beta$  in vitro and cultured primary neurons [18]. However, the relative contribution of PKA or other kinases to the phosphorylation of A $\beta$  in human brain is not known. It is also possible that a decrease in phosphatase activities could contribute to the accumulation of phosphorylated A $\beta$  species during the pathogenesis of AD and DS.

Studies in vitro, with cultured neurons, and *Drosophila* models showed that phosphorylation promotes the aggregation and increases toxicity of A $\beta$  [18, 26]. However, in human brains, pSer8A $\beta$  deposition is detected predominantly in the symptomatic phase of AD [40, 42], when a considerable degree of synapse loss has already occurred. Thus, it will be interesting to investigate whether pSer8A $\beta$  and other A $\beta$  variants initiate neuronal damage as soluble species. Indeed, soluble oligomeric A $\beta$  species are considered to exert higher neurotoxicity as compared to fibrillar assemblies in extracellular plaques [67–69].

We also demonstrate the deposition of pSer8A $\beta$  in a variety of AD Tg mouse models. Mouse models of AD that accurately recapitulate major characteristics of A $\beta$  pathology are critical for better understanding molecular mechanisms of pathogenesis, and to assess novel therapeutics in preclinical studies [43–47]. Most of these models have been generated by transgenic overexpression of the gene encoding human APP (alone or in combination with human *PSEN1* or human *MAPT*), and present with progressive accumulation of A $\beta$  in form of extracellular plaques and neurofibrillary tangles. Some of these Tg mouse models develop CAA to various degrees, which allow studying the effect of A $\beta$  accumulation on vascular function [46, 70, 71]. These transgenic models use various promoters to drive transgene expression in different genetic back grounds (Table 2). Interestingly, such mouse models showed that neuronal A $\beta$  generation could drive CAA [72], and impaired A $\beta$  clearance seems to enhance CAA [73]. Our study supports a critical role of A $\beta$  generated by neurons in the formation of CAA, as abundant CAA was observed in transgenic mice with APP expression controlled by the neuron-specific *Thy-1*, *Prnp* or *PDGF $\beta$*  promoters (Table 2), although minor contribution of A $\beta$  generated by additional brain cells cannot be excluded. Early onset (~ 3 months of age) and progressive accumulation of CAA is observed in the

TgSwDI model with three autosomal dominant mutations (Swedish; Dutch; Iowa), but not in 4 or 5 month old J20 or 3xTg-AD mice. The accelerated deposition of A $\beta$  in CAA in the TgSwDI model is in line with previous reports, and supports a critical role of the amino acid sequence and structure of A $\beta$  in CAA formation [50, 70]. The Dutch and Iowa mutations are associated with extensive CAA but limited plaque pathology [74, 75].

In all transgenic mouse models investigated here, CAA contained npA $\beta$  and pSer8A $\beta$ , indicating co-deposition of these variants. In a previous study, we showed co-deposition of phosphorylated and non-phosphorylated A $\beta$  in the preclinical and clinical phase of AD [40]. However, about 30 to 40% of cases with CAA did not show pSer8A $\beta$  [40], indicating a larger heterogeneity in the development of CAA in the human brain as compared to that of transgenic mouse models. As also demonstrated in this study, all investigated transgenic mouse models showed co-deposition of npA $\beta$  and pSer8A $\beta$  in extracellular plaques apparently already at early phases of A $\beta$  deposition in the respective model. The overall load pSer8A $\beta$  in the transgenic mouse models appears to mainly depend on the extent of total A $\beta$  generation determined by the individual mutations in APP or PS1. This is consistent with previous reports with other transgenic mouse models [18, 37]. However, as shown here and in previous studies [40, 42], only a subset of brains from human cases with A $\beta$  plaque pathology, especially in the pathological preclinical phase of AD present with pSer8A $\beta$  deposition. Together, these data on one hand show similarities in the deposition of modified and unmodified A $\beta$  species, but on the other hand also demonstrate considerable differences in the composition of A $\beta$  deposits during the pathogenesis of human AD and  $\beta$ -amyloidosis in transgenic mouse models.

## Conclusions

Previous studies showed that amyloid deposits of AD and DS brains are heterogeneous, and could contain post-translationally modified and truncated A $\beta$  variants [16, 18–23, 29, 31, 35, 36, 39, 42, 54, 61, 76]. Some of these modified A $\beta$  species are also observed in the brains of transgenic mice. These A $\beta$  modifications are of particular interest because they could contribute to the deposition of A $\beta$  by altering A $\beta$  conformation, aggregation and the proteolytic degradation by neuropeptidases. Thus, the comparative analysis of the spatiotemporal deposition of pSer8A $\beta$  and other modified or unmodified A $\beta$  species, and the relative composition of characteristic A $\beta$  deposits in form of extracellular plaques and cerebral amyloid angiopathy could be relevant for better understanding the onset and progression of AD and AD like pathology in DS, and to identify specific A $\beta$  species for diagnosis and therapeutic targeting.

## Supplementary information

Supplementary information accompanies this paper at <https://doi.org/10.1186/s40478-020-00959-w>.

**Additional file 1: Supplementary Figure 1. Specificity of phosphorylation-state specific A $\beta$  antibodies.** SDS-PAGE electrophoresis and immunoblotting of non-modified full length (A $\beta$ 1–40/42), truncated (A $\beta$ 3–40/42), phosphorylated (pSer8A $\beta$ 1–40/42, pSer26A $\beta$ 1–40, pSer8A $\beta$ 3–40/42, pSer26A $\beta$ 3–40/42), pyroglutaminated A $\beta$  (pyroA $\beta$ 3–40/42) or nitrated A $\beta$  (NitroA $\beta$ 1–42) variants with 1E4E11 (pSer8A $\beta$ -specific) and 7H3D6 (npA $\beta$ -specific) antibodies. 1E4E11 specifically recognized phosphorylated Ser-8 full-length (1–40/42) and truncated pSer8A $\beta$ 3–40/42 variants, whereas 7H3D6 antibody demonstrated no reactivity against A $\beta$  peptides phosphorylated at Ser-8 residue and specifically detects only full-length A $\beta$ 1–40/42 variants without N-terminal modifications. Generic 4G8-antibody (epitope 17–24) recognizes all examined A $\beta$  variants.

**Additional file 2: Supplementary Figure 2. pSer8A $\beta$  and npA $\beta$  deposition in parenchyma, leptomeningeal blood vessels and intraneuronally in different Tg mouse models.**

Immunohistochemistry of 16 months old J20 (a-d), 14 month-old hAPP751 (e-h), 18 month-old PS/APP (i-l), and 27 month-old 3xTg-AD (m-p) mouse brain tissue demonstrates the presence of pSer8A $\beta$  in leptomeningeal and parenchymal blood vessels in addition to extracellular amyloid plaques in J20, hAPP751 and PS/APP mouse brains, and extracellular and intraneuronal accumulation of npA $\beta$  and pSer8A $\beta$  in the neocortex in 3xTg-AD mice. Boxes in images a, b, e, f, i, j, m and n (scale bar = 200  $\mu$ m) are enlarged in c, d, g, h, k, l, o and p (scale bar = 50  $\mu$ m).

## Abbreviations

AD: Alzheimer's disease; A $\beta$ : Amyloid-beta peptide; AC: Aged control; APP: Amyloid precursor protein; CAA: Cerebral amyloid angiopathy; DS: Down syndrome; FAD: Familial Alzheimer's disease; mAb: monoclonal antibody; MAPT: Microtubule-associated protein tau; npA $\beta$ : Non-phosphorylated A $\beta$ ; pSer8A $\beta$ : Phosphorylated Serine-8 A $\beta$ ; PS: Presenilin

## Acknowledgments

We kindly thank Jeffrey L. Frost and Kevin X. Le for technical assistance. We thank Dr. Susanne Schoch McGovern and Silvia Cases for the use and technical assistance on microscopy. We thank the following individuals for generously providing breeder mice or mouse brains sections: Dr. William E. Van Nostrand (George & Anne Ryan Institute for Neuroscience and Department of Biomedical and Pharmaceutical Sciences, University of Rhode Island, Kingston, USA) provided APPSwdI mouse brain sections; Dr. Eliezer Masliah (Division of Neurosciences, National Institute on Aging, National Institutes of Health, Bethesda, USA) provided hAPP751 mouse brain sections; Dr. Karen Duff (UCL, London, UK) provided PSAPP mouse brain sections; Dr. Lennart Mucke (Gladstone Institute, University of California, San Francisco, CA, USA) provided J20 breeder mice; Dr. Frank M. LaFerla (University of California, Irvine, CA, USA) provided 3xTg-AD breeders. APP/PS1dE9 mice were purchased from Jackson Laboratories, Bar Harbor, ME, USA. We also thank Dr. Elizabeth Head (University of California, Irvine, CA, USA) for providing comments on the manuscript. We acknowledge support from Alzheimer Forschung Initiative e.V for Open Access Publishing.

## Authors' contributions

SK, JW and CAL designed the study. SK performed the immunostainings, analysed the data and wrote the paper. JW and CAL contributed to data analyses, interpretations and implications. The manuscript was read, edited and approved by all authors.

## Funding

This work was funded by Deutsche Forschungsgemeinschaft (grant #WA1477/6–3 (JW)), the Alzheimer Forschungs Initiative (grants #12854 and #17011 (SK)), the NIH/NIA (R01 AG040092 and R01/RF1 AG058657 (CAL)).

## Availability of data and materials

All data generated or analyzed during this study are included in this article and its supplementary files.

**Ethics approval and consent to participate**

Human brain tissue was collected at the time of autopsy, having obtained prior consent from the next of kin and following protocols approved by the Partners Human Research Committee at Brigham and Women's Hospital (Boston, MA, USA). All procedures and use of mice at Brigham and Women's Hospital was approved by the Harvard Medical Area Standing Committee on animals and was in compliance with state and federal regulations.

**Consent for publication**

Not applicable.

**Competing interests**

The authors declare that they have no competing or conflict of interests.

Received: 17 April 2020 Accepted: 30 May 2020

Published online: 29 July 2020

**References**

- Montine TJ, Phelps CH, Beach TG, Bigio EH, Cairns NJ, Dickson DW, Duyckaerts C, Frosch MP, Masliah E, Mirra SS, Nelson PT, Schneider JA, Thal DR, Trojanowski JQ, Vinters HV, Hyman BT (2012) National Institute on Aging-Alzheimer's association guidelines for the neuropathologic assessment of Alzheimer's disease: a practical approach. *Acta Neuropathol* 123(1):1–11 <https://doi.org/10.1007/s00401-011-0910-3>
- Duyckaerts C, Delatour B, Potier M-C (2009) Classification and basic pathology of Alzheimer disease. *Acta Neuropathol* 118(1):5–36 <https://doi.org/10.1007/s00401-009-0532-1>
- Alafuzoff I, Thal DR, Arzberger T, Bogdanovic N, Al-Sarraj S, Bodi I, Boluda S, Bugiani O, Duyckaerts C, Gelpi E, Gentleman S, Giaccone G, Graeber M, Hortobagyi T, Höftberger R, Ince P, Ironside JW, Kavantzias N, King A, Korkolopoulou P, Kovács GG, Meyronet D, Monoranu C, Nilsson T, Parchi P, Patsouris E, Pikkarainen M, Revesz T, Rozemuller A, Seilhean D et al (2009) Assessment of  $\beta$ -amyloid deposits in human brain: a study of the BrainNet Europe Consortium. *Acta Neuropathol* 117(3):309–320 <https://doi.org/10.1007/s00401-009-0485-4>
- Selkoe DJ, Hardy J (2016) The amyloid hypothesis of Alzheimer's disease at 25 years. *EMBO Mol Med* 8(6):595–608 [10.15252/emmm.201606210](https://doi.org/10.15252/emmm.201606210)
- Oikawa N, Walter J (2019) Presenilins and  $\gamma$ -Secretase in membrane Proteostasis. *Cells* 8(3) <https://doi.org/10.3390/cells8030209>
- Haass C, Kaether C, Thinakaran G, Sisodia S (2012) Trafficking and proteolytic processing of APP. *Cold Spring Harb Perspect Med* 2(5):a006270 <https://doi.org/10.1101/cshperspect.a006270>
- Walter S, Jumpertz T, Hüttenrauch M, Ogorek I, Gerber H, Storck SE, Zampar S, Dimitrov M, Lehmann S, Lepka K, Berndt C, Wiltfang J, Becker-Pauly C, Behr D, Pietrzik CU, Fraering PC, Wirths O, Weggen S (2019) The metalloprotease ADAMTS4 generates N-truncated A $\beta$ 4-x species and marks oligodendrocytes as a source of amyloidogenic peptides in Alzheimer's disease. *Acta Neuropathol* 137(2):239–257 <https://doi.org/10.1007/s00401-018-1929-5>
- Tekirian TL, Saido TC, Markesbery WR, Russell MJ, Wekstein DR, Patel E, Geddes JW (1998) N-terminal heterogeneity of parenchymal and cerebrovascular Abeta deposits. *J Neuropathol Exp Neurol* 57(1):76–94 <https://doi.org/10.1097/00005072-199801000-00009>
- Saito T, Suemoto T, Brouwers N, Slegers K, Funamoto S, Mihira N, Matsuba Y, Yamada K, Nilsson P, Takano J, Nishimura M, Iwata N, van Broeckhoven C, Ihara Y, Saido TC (2011) Potent amyloidogenicity and pathogenicity of A $\beta$ 43. *Nat Neurosci* 14(8):1023–1032 <https://doi.org/10.1038/nn.2858>
- Saido TC, Yamao-Harigaya W, Iwatsubo T, Kawashima S (1996) Amino- and carboxyl-terminal heterogeneity of beta-amyloid peptides deposited in human brain. *Neurosci Lett* 215(3):173–176. [https://doi.org/10.1016/0304-3940\(96\)12970-0](https://doi.org/10.1016/0304-3940(96)12970-0)
- García-González L, Pilat D, Baranger K, Rivera S (2019) Emerging alternative proteinases in APP metabolism and Alzheimer's disease pathogenesis: a focus on MT1-MMP and MT5-MMP. *Front Aging Neurosci* 11:244 <https://doi.org/10.3389/fnagi.2019.00244>
- Dunys J, Valverde A, Checler F (2018) Are N- and C-terminally truncated A $\beta$  species key pathological triggers in Alzheimer's disease? *J Biol Chem* 293(40):15419–15428 <https://doi.org/10.1074/jbc.R118.003999>
- Becker-Pauly C, Pietrzik CU (2017) The Metalloprotease Meprin  $\beta$  is an alternative  $\beta$ -Secretase of APP. *Front Mol Neurosci* 9 <https://doi.org/10.3389/fnmol.2016.00159>
- Shimizu T, Watanabe A, Ogawara M, Mori H, Shirasawa T (2000) Isoaspartate formation and neurodegeneration in Alzheimer's disease. *Arch Biochem Biophys* 381(2):225–234 <https://doi.org/10.1006/abbi.2000.1955>
- Schilling S, Zeitschel U, Hoffmann T, Heiser U, Francke M, Kehlen A, Holzer M, Hutter-Paier B, Prokesch M, Windisch M, Jagla W, Schlenzig D, Lindner C, Rudolph T, Reuter G, Cynis H, Montag D, Demuth H-U, Rossner S (2008) Glutaminyl cyclase inhibition attenuates pyroglutamate Abeta and Alzheimer's disease-like pathology. *Nat Med* 14(10):1106–1111 <https://doi.org/10.1038/nm.1872>
- Saido TC, Iwatsubo T, Mann DM, Shimada H, Ihara Y, Kawashima S (1995) Dominant and differential deposition of distinct beta-amyloid peptide species, a beta N3(pE), in senile plaques. *Neuron* 14(2):457–466. [https://doi.org/10.1016/0896-6273\(95\)90301-1](https://doi.org/10.1016/0896-6273(95)90301-1)
- Kummer MP, Hermes M, Delekarte A, Hammerschmidt T, Kumar S, Terwel D, Walter J, Pape H-C, König S, Roeder S, Jessen F, Klockgether T, Korte M, Heneka MT (2011) Nitration of tyrosine 10 critically enhances amyloid beta aggregation and plaque formation. *Neuron* 71(5):833–844 <https://doi.org/10.1016/j.neuron.2011.07.001>
- Kumar S, Rezaei-Ghaleh N, Terwel D, Thal DR, Richard M, Hoch M, Mc Donald JM, Wullner U, Glebov K, Heneka MT, Walsh DM, Zweckstetter M, Walter J (2011) Extracellular phosphorylation of the amyloid beta-peptide promotes formation of toxic aggregates during the pathogenesis of Alzheimer's disease. *EMBO J* 30(11):2255–2265 <https://doi.org/10.1038/emboj.2011.138>
- Kumar S, Wirths O, Stuber K, Wunderlich P, Koch P, Theil S, Rezaei-Ghaleh N, Zweckstetter M, Bayer TA, Brustle O, Thal DR, Walter J (2016) Phosphorylation of the amyloid beta-peptide at Ser26 stabilizes oligomeric assembly and increases neurotoxicity. *Acta Neuropathol* 131(4):525–537 <https://doi.org/10.1007/s00401-016-1546-0>
- Frost JL, Le KX, Cynis H, Ekpo E, Kleinschmidt M, Palmour RM, Ervin FR, Snigdha S, Cotman CW, Saido TC, Vassar RJ, St George-Hyslop P, Ikezu T, Schilling S, Demuth H-U, Lemere CA (2013) Pyroglutamate-3 amyloid-beta deposition in the brains of humans, non-human primates, canines, and Alzheimer disease-like transgenic mouse models. *Am J Pathol* 183(2):369–381 <https://doi.org/10.1016/j.ajpath.2013.05.005>
- Bayer TA, Wirths O (2014) Focusing the amyloid cascade hypothesis on N-truncated Abeta peptides as drug targets against Alzheimer's disease. *Acta Neuropathol* 127(6):787–801 <https://doi.org/10.1007/s00401-014-1287-x>
- Roher AE, Kokjohn TA, Clarke SG, Sierks MR, Maarouf CL, Serrano GE, Sabbagh MS, Beach TG (2017) APP/A $\beta$  structural diversity and Alzheimer's disease pathogenesis. *Neurochem Int* 110:1–13 <https://doi.org/10.1016/j.neuint.2017.08.007>
- Wirths O, Zampar S (2019) Emerging roles of N- and C-terminally truncated A $\beta$  species in Alzheimer's disease. *Expert Opin Ther Targets* 23(12):991–1004 <https://doi.org/10.1080/14728222.2019.1702972>
- Thal DR, Walter J, Saido TC, Fandrich M (2015) Neuropathology and biochemistry of Abeta and its aggregates in Alzheimer's disease. *Acta Neuropathol* 129(2):167–182 <https://doi.org/10.1007/s00401-014-1375-y>
- Rezaei-Ghaleh N, Amininasab M, Kumar S, Walter J, Zweckstetter M (2016) Phosphorylation modifies the molecular stability of beta-amyloid deposits. *Nat Commun* 7:11359 <https://doi.org/10.1038/ncomms11359>
- Kumar S, Walter J (2011) Phosphorylation of amyloid beta (Abeta) peptides - a trigger for formation of toxic aggregates in Alzheimer's disease. *Aging* 3(8):803–812. <https://doi.org/10.18632/aging.100362>
- Kumar S, Singh S, Hinze D, Josten M, Sahl H-G, Siepmann M, Walter J (2012) Phosphorylation of amyloid-beta peptide at serine 8 attenuates its clearance via insulin-degrading and angiotensin-converting enzymes. *J Biol Chem* 287(11):8641–8651 <https://doi.org/10.1074/jbc.M111.279133>
- Barykin EP, Mitkevich VA, Kozin SA, Makarov AA (2017) Amyloid  $\beta$  modification: a key to the sporadic Alzheimer's disease? *Front Genet* 8 <https://doi.org/10.3389/fgene.2017.00058>
- Lott IT, Head E (2019) Dementia in Down syndrome: unique insights for Alzheimer disease research. *Nat Rev Neurol* 15(3):135–147 <https://doi.org/10.1038/s41582-018-0132-6>
- Head E, Lott IT, Wilcock DM, Lemere CA (2016) Aging in Down syndrome and the development of Alzheimer's disease neuropathology. *Curr Alzheimer Res* 13(1):18–29 <https://doi.org/10.2174/1567205012666151020114607>
- Abrahamson EE, Head E, Lott IT, Handen BL, Mufson EJ, Christian BT, Klunk WE, Ikonomic MD (2019) Neuropathological correlates of amyloid PET

- imaging in Down syndrome. *Dev Neurobiol* 79(7):750–766 <https://doi.org/10.1002/dneu.22713>
32. Teller JK, Russo C, DeBusk LM, Angelini G, Zaccaro D, Dagna-Bricarelli F, Scartezzini P, Bertolini S, Mann DM, Tabaton M, Gambetti P (1996) Presence of soluble amyloid beta-peptide precedes amyloid plaque formation in Down's syndrome. *Nat Med* 2(1):93–95 <https://doi.org/10.1038/nm0196-93>
  33. Mori C, Spooner ET, Wisniewski KE, Wisniewski TM, Yamaguchi H, Saido TC, Tolan DR, Selkoe DJ, Lemere CA (2002) Intraneuronal Abeta42 accumulation in Down syndrome brain. *Amyloid* 9(2):88–102 <https://doi.org/10.3109/13506120208995241>
  34. Davidson YS, Robinson A, Prasher VP, Mann DMA (2018) The age of onset and evolution of Braak tangle stage and Thal amyloid pathology of Alzheimer's disease in individuals with Down syndrome. *Acta Neuropathol Commun* 6 <https://doi.org/10.1186/s40478-018-0559-4>
  35. Lemere CA, Blusztajn JK, Yamaguchi H, Wisniewski T, Saido TC, Selkoe DJ (1996) Sequence of deposition of heterogeneous amyloid beta-peptides and APO E in Down syndrome: implications for initial events in amyloid plaque formation. *Neurobiol Dis* 3(1):16–32 <https://doi.org/10.1006/mbdi.1996.0003>
  36. Liu K, Solano I, Mann D, Lemere C, Mercken M, Trojanowski JQ, Lee VM-Y (2006) Characterization of Abeta11–40/42 peptide deposition in Alzheimer's disease and young Down's syndrome brains: implication of N-terminally truncated Abeta species in the pathogenesis of Alzheimer's disease. *Acta Neuropathol* 112(2):163–174 <https://doi.org/10.1007/s00401-006-0077-5>
  37. Kumar S, Wirths O, Theil S, Gerth J, Bayer TA, Walter J (2013) Early intraneuronal accumulation and increased aggregation of phosphorylated Abeta in a mouse model of Alzheimer's disease. *Acta Neuropathol* 125(5):699–709 <https://doi.org/10.1007/s00401-013-1107-8>
  38. Rezaei-Ghaleh N, Kumar S, Walter J, Zweckstetter M (2016) Phosphorylation interferes with maturation of amyloid-beta fibrillar structure in the N terminus. *J Biol Chem* 291(31):16059–16067 <https://doi.org/10.1074/jbc.M116.728956>
  39. Ashby EL, Miners JS, Kumar S, Walter J, Love S, Kehoe PG (2015) Investigation of Abeta phosphorylated at serine 8 (pAbeta) in Alzheimer's disease, dementia with Lewy bodies and vascular dementia. *Neuropathol Appl Neurobiol* 41(4):428–444 <https://doi.org/10.1111/nan.12212>
  40. Gerth J, Kumar S, Rijal Upadhaya A, Ghebremedhin E, von Arnim CAF, Thal DR, Walter J (2018) Modified amyloid variants in pathological subgroups of  $\beta$ -amyloidosis. *Ann Clin Transl Neurol* 5(7):815–831 <https://doi.org/10.1002/acn3.577>
  41. Kumar S, Frost JL, Cotman CW, Head E, Palmour R, Lemere CA, Walter J (2018) Deposition of phosphorylated amyloid- $\beta$  in brains of aged nonhuman primates and canines. *Brain Pathol* 28(3):427–430 <https://doi.org/10.1111/bpa.12573>
  42. Rijal Upadhaya A, Kosterin I, Kumar S, von Arnim CAF, Yamaguchi H, Fandrich M, Walter J, Thal DR (2014) Biochemical stages of amyloid-beta peptide aggregation and accumulation in the human brain and their association with symptomatic and pathologically preclinical Alzheimer's disease. *Brain* 137(Pt 3):887–903 <https://doi.org/10.1093/brain/awt362>
  43. Jankowsky JL, Zheng H (2017) Practical considerations for choosing a mouse model of Alzheimer's disease. *Mol Neurodegener* 12(1):89 <https://doi.org/10.1186/s13024-017-0231-7>
  44. Sasaguri H, Nilsson P, Hashimoto S, Nagata K, Saito T, de Strooper B, Hardy J, Vassar R, Winblad B, Saido TC (2017) APP mouse models for Alzheimer's disease preclinical studies. *EMBO J* 36(17):2473–2487. <https://doi.org/10.15252/emboj.201797397>
  45. Webster SJ, Bachstetter AD, Nelson PT, Schmitt FA, van Eldik LJ (2014) Using mice to model Alzheimer's dementia: an overview of the clinical disease and the preclinical behavioral changes in 10 mouse models. *Front Genet* 5 <https://doi.org/10.3389/fgene.2014.00088>
  46. Drummond E, Wisniewski T (2017) Alzheimer's disease: experimental models and reality. *Acta Neuropathol* 133(2):155–175 <https://doi.org/10.1007/s00401-016-1662-x>
  47. Braidy N, Munoz P, Palacios AG, Castellano-Gonzalez G, Inestrosa NC, Chung RS, Sachdev P, Guillemin GJ (2012) Recent rodent models for Alzheimer's disease: clinical implications and basic research. *J Neural Transm (Vienna)* 119(2):173–195 <https://doi.org/10.1007/s00702-011-0731-5>
  48. Mucke L, Masliah E, Yu GQ, Mallory M, Rockenstein EM, Tatsuno G, Hu K, Kholodenko D, Johnson-Wood K, McConlogue L (2000) High-level neuronal expression of abeta 1–42 in wild-type human amyloid protein precursor transgenic mice: Synaptotoxicity without plaque formation. *J Neurosci* 20(11):4050–4058 <https://doi.org/10.1523/JNEUROSCI.20-11-04050.2000>
  49. Rockenstein E, Mallory M, Mante M, Sisk A, Masliah E (2001) Early formation of mature amyloid-beta protein deposits in a mutant APP transgenic model depends on levels of Abeta (1–42). *J Neurosci Res* 66(4):573–582 <https://doi.org/10.1002/jnr.1247>
  50. Davis J, Xu F, Deane R, Romanov G, Previti ML, Zeigler K, Zlokovic BV, van Nostrand WE (2004) Early-onset and robust cerebral microvascular accumulation of amyloid beta-protein in transgenic mice expressing low levels of a vasculotropic Dutch/lowa mutant form of amyloid beta-protein precursor. *J Biol Chem* 279(19):20296–20306 <https://doi.org/10.1074/jbc.M312946200>
  51. Jankowsky JL, Slunt HH, Ratovitski T, Jenkins NA, Copeland NG, Borchelt DR (2001) Co-expression of multiple transgenes in mouse CNS: a comparison of strategies. *Biomol Eng* 17(6):157–165 [https://doi.org/10.1016/s1389-0344\(01\)00067-3](https://doi.org/10.1016/s1389-0344(01)00067-3)
  52. Holcomb L, Gordon MN, McGowan E, Yu X, Benkovic S, Jantzen P, Wright K, Saad I, Mueller R, Morgan D, Sanders S, Zehr C, O'Campo K, Hardy J, Prada CM, Eckman C, Younkin S, Hsiao K, Duff K (1998) Accelerated Alzheimer-type phenotype in transgenic mice carrying both mutant amyloid precursor protein and presenilin 1 transgenes. *Nat Med* 4(1):97–100 <https://doi.org/10.1038/nm0198-097>
  53. Oddo S, Caccamo A, Shepherd JD, Murphy MP, Golde TE, Kaye R, Metherate R, Mattson MP, Akbari Y, LaFerla FM (2003) Triple-transgenic model of Alzheimer's disease with plaques and tangles: intracellular Abeta and synaptic dysfunction. *Neuron* 39(3):409–421. [https://doi.org/10.1016/S0896-6273\(03\)00434-3](https://doi.org/10.1016/S0896-6273(03)00434-3)
  54. Hosoda R, Saido TC, Otvos L, Arai T, Mann DM, Lee VM, Trojanowski JQ, Iwatsubo T (1998) Quantification of modified amyloid beta peptides in Alzheimer disease and Down syndrome brains. *J Neuropathol Exp Neurol* 57(11):1089–1095 <https://doi.org/10.1097/00005072-199811000-00012>
  55. Iwatsubo T, Saido TC, Mann DM, Lee VM, Trojanowski JQ (1996) Full-length amyloid-beta (1–42(43)) and amino-terminally modified and truncated amyloid-beta 42(43) deposit in diffuse plaques. *Am J Pathol* 149(6):1823–1830
  56. Jankowsky JL, Fadale DJ, Anderson J, Xu GM, Gonzales V, Jenkins NA, Copeland NG, Lee MK, Younkin LH, Wagner SL, Younkin SG, Borchelt DR (2004) Mutant presenilins specifically elevate the levels of the 42 residue beta-amyloid peptide in vivo: evidence for augmentation of a 42-specific gamma secretase. *Hum Mol Genet* 13(2):159–170 <https://doi.org/10.1093/hmg/ddh019>
  57. Takeuchi A, Irizarry MC, Duff K, Saido TC, Hsiao AS, Hasegawa M, Mann DM, Hyman BT, Iwatsubo T (2000) Age-related amyloid beta deposition in transgenic mice overexpressing both Alzheimer mutant presenilin 1 and amyloid beta precursor protein Swedish mutant is not associated with global neuronal loss. *Am J Pathol* 157(1):331–339. [https://doi.org/10.1016/s0002-9440\(10\)64544-0](https://doi.org/10.1016/s0002-9440(10)64544-0)
  58. LaFerla FM, Green KN, Oddo S (2007) Intracellular amyloid-beta in Alzheimer's disease. *Nat Rev Neurosci* 8(7):499–509 <https://doi.org/10.1038/nrn2168>
  59. Billings LM, Oddo S, Green KN, McLaugh JL, LaFerla FM (2005) Intraneuronal Abeta causes the onset of early Alzheimer's disease-related cognitive deficits in transgenic mice. *Neuron* 45(5):675–688 <https://doi.org/10.1016/j.neuron.2005.01.040>
  60. Takahashi RH, Nagao T, Gouras GK (2017) Plaque formation and the intraneuronal accumulation of beta-amyloid in Alzheimer's disease. *Pathol Int* 67(4):185–193. <https://doi.org/10.1111/pin.12520a>
  61. Miravalle L, Calero M, Takao M, Roher AE, Ghetti B, Vidal R (2005) Amino-terminally truncated Abeta peptide species are the main component of cotton wool plaques. *Biochemistry* 44(32):10810–10821 <https://doi.org/10.1021/bi0508237>
  62. Cabrera E, Mathews P, Mezhericher E, Beach TG, Deng J, Neubert TA, Rostagno A, Ghiso J (2018) A $\beta$  truncated species: Implications for brain clearance mechanisms and amyloid plaque deposition. *Biochim Biophys Acta Mol Basis Dis* 1864(1):208–225 <https://doi.org/10.1016/j.bbadis.2017.07.005>
  63. Chung S-H (2009) Aberrant phosphorylation in the pathogenesis of Alzheimer's disease. *BMB Rep* 42(8):467–474 <https://doi.org/10.5483/bmbrep.2009.42.8.467>
  64. Weitzdoerfer R, Toran N, Subramanian S, Pollak A, Dierssen M, Lubec G (2015) A cluster of protein kinases and phosphatases modulated in fetal Down syndrome (trisomy 21) brain. *Amino Acids* 47(6):1127–1134 <https://doi.org/10.1007/s00726-015-1941-1>
  65. Braithwaite SP, Stock JB, Lombroso PJ, Nairn AC (2012) Protein phosphatases and Alzheimer's disease. *Prog Mol Biol Transl Sci* 106:343–379 <https://doi.org/10.1016/B978-0-12-396456-4.00012-2>

66. Rosenberger AFN, Hilhorst R, Coart E, García Barrado L, Naji F, Rozemuller AJM, van der Flier WM, Scheltens P, Hoozemans JJM, van der Vies SM (2016) Protein Kinase Activity Decreases with Higher Braak Stages of Alzheimer's Disease Pathology. *J Alzheimers Dis* 49(4):927–943 <https://doi.org/10.3233/JAD-150429>
67. Cline EN, Bicca MA, Viola KL, Klein WL The Amyloid- $\beta$  Oligomer Hypothesis: Beginning of the Third Decade. *J Alzheimers Dis* 64(Suppl 1):S567–S610 <https://doi.org/10.3233/JAD-179941>
68. Li S, Selkoe DJ (2020) A mechanistic hypothesis for the impairment of synaptic plasticity by soluble A $\beta$  oligomers from Alzheimer's brain. *J Neurochem*. <https://doi.org/10.1111/jnc.15007>
69. Haass C, Selkoe DJ (2007) Soluble protein oligomers in neurodegeneration: lessons from the Alzheimer's amyloid beta-peptide. *Nat Rev Mol Cell Biol*. 8(2):101–112. <https://doi.org/10.1038/nrm2101>
70. Jäkel L, van Nostrand WE, Nicoll JAR, Werring DJ, Verbeek MM (2017) Animal models of cerebral amyloid angiopathy. *Clin Sci* 131(19):2469–2488 <https://doi.org/10.1042/CS20170033>
71. Klohs J, Rudin M, Shimshek DR, Beckmann N (2014) Imaging of cerebrovascular pathology in animal models of Alzheimer's disease. *Front Aging Neurosci* 6:32 <https://doi.org/10.3389/fnagi.2014.00032>
72. Calhoun ME, Burgermeister P, Phinney AL, Stalder M, Tolnay M, Wiederhold KH, Abramowski D, Sturchler-Pierrat C, Sommer B, Staufenbiel M, Jucker M (1999) Neuronal overexpression of mutant amyloid precursor protein results in prominent deposition of cerebrovascular amyloid. *Proc Natl Acad Sci U S A* 96(24):14088–14093 <https://doi.org/10.1073/pnas.96.24.14088>
73. Herzig MC, van Nostrand WE, Jucker M (2006) Mechanism of cerebral beta-amyloid angiopathy: murine and cellular models. *Brain Pathol* 16(1):40–54 <https://doi.org/10.1111/j.1750-3639.2006.tb00560.x>
74. Kamp JA, Moursel LG, Haan J, Terwindt GM, Lesnik Oberstein SAMJ, van Duinen SG, van Roon-Mom WMC (2014) Amyloid  $\beta$  in hereditary cerebral hemorrhage with amyloidosis-Dutch type. *Rev Neurosci* 25(5):641–651 <https://doi.org/10.1515/revneuro-2014-0008>
75. Grabowski TJ, Cho HS, Vonsattel JP, Rebeck GW, Greenberg SM (2001) Novel amyloid precursor protein mutation in an Iowa family with dementia and severe cerebral amyloid angiopathy. *Ann Neurol* 49(6):697–705 <https://doi.org/10.1002/ana.1009>
76. Russo C, Saido TC, DeBusk LM, Tabaton M, Gambetti P, Teller JK (1997) Heterogeneity of water-soluble amyloid beta-peptide in Alzheimer's disease and Down's syndrome brains. *FEBS Lett* 409(3):411–416 [https://doi.org/10.1016/s0014-5793\(97\)00564-4](https://doi.org/10.1016/s0014-5793(97)00564-4)

## Publisher's Note

Springer Nature remains neutral with regard to jurisdictional claims in published maps and institutional affiliations.

**Ready to submit your research? Choose BMC and benefit from:**

- fast, convenient online submission
- thorough peer review by experienced researchers in your field
- rapid publication on acceptance
- support for research data, including large and complex data types
- gold Open Access which fosters wider collaboration and increased citations
- maximum visibility for your research: over 100M website views per year

**At BMC, research is always in progress.**

Learn more [biomedcentral.com/submissions](https://biomedcentral.com/submissions)

